Gearbox Ripple Rejection of Robots Using Observer and Adaptive Control Theory

Sebastian Maier * **Johann Bals** ** **Marc Bodson** ***

* *Department of System Dynamics and Control, Institute of Robotics and Mechatronics, German Aerospace Center (DLR), 82234 Wessling, Germany, Muenchner Str. 20, (e-mail: Sebastian.Maier@dlr.de)*
** *Department of System Dynamics and Control, Institute of Robotics and Mechatronics, German Aerospace Center (DLR), 82234 Wessling, Germany, Muenchner Str. 20, (e-mail: Johann.Bals@dlr.de).*
*** *Department of Electrical and Computer Engineering, University of Utah 50 S Central Campus Dr., Salt Lake City, UT 84112, USA, (e-mail: bodson@ece.utah.edu)*

Abstract: Robots are often run with permanent magnet synchronous motors (PMSM) with a high ratio gearbox. Both parts can produce parasitic oscillations (ripples), which let the robot shake at tool center point. The gearbox ripple problem is more complicated to be solved with control theory because only motor side sensors should be used. Due to the internal model principle gearbox side information is necessary to solve the problem. The first algorithm uses an observer to get gearbox side information where the second algorithm uses a gearbox side rate sensor. The algorithms are tested with a nonlinear SISO problem and with a nonlinear MIMO system.
In both cases the ripples are canceled with an adaptive controller which estimates the phase and magnitude of the ripple. This adaptive controller is designed separately and is added to the existing basis controller. The algorithms are tested in simulation and on a testbed, which is an industrial application.

1. INTRODUCTION

One goal in robotic applications is that the robot does not oscillate at the tool center point during an operating process like laser welding or gluing. These oscillations are generated by the motors and by the gearboxes of the robot. In this paper we consider only the gearbox ripples, which occur due to fabrication tolerances and result in a non-ideal ratio, see Teijin-Seiki [2010] and Sumitomo [1996].
The gearbox ripples are complicated to reject because gearbox side information is needed. The main topic of the paper is to design an observer for a nonlinear MIMO system, which can estimate the system states correctly. For the linear SISO case, in the field of vibration control, an observer is designed by Bohn et al. [2005]. In robotic applications an observer is designed by Kurze [2008], but here mostly a decoupled observer is studied which has not an internal model of the ripple.
To reject the observed or measured ripple adaptive control is used. This paper does not give a deep insight into the theory of adaptive control. Mainly the controllers were developed by Bodson and Douglas [1997] and Guo and Bodson [2010]. For the MIMO case, see Wu and Bodson [2004] and the controllers are successfully tested on a mechatronical system, see Maier and Bodson [2008].

2. MULTIBODY DYNAMICS OF A ROBOT

There are several possibilities to derive the equations of motion for a rigid link elastic joint robot, see Pfeiffer [1989], Spong and Vidyasagar [1989] and de Wit et al. [1996], so here only the very basic equations are given. The methode of Lagrange uses a vector of the generalized coordinates $\boldsymbol{q} = [q_1\ q_2\ q_3\ q_4\ q_5\ q_6]$, where the index represents the axis of the robot, see figure 1. The Lagrange function is given by

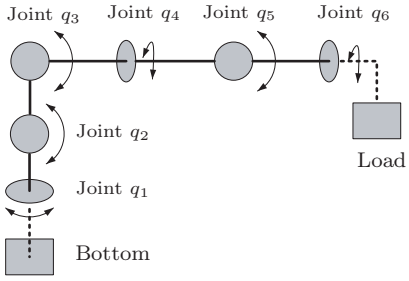

Fig. 1. Kinematics of the robot.

$$\mathcal{L} = \mathcal{T}(\dot{\boldsymbol{q}}, \boldsymbol{q}) - \mathcal{U}(\boldsymbol{q}) \tag{1}$$

with the kinetic energy $\mathcal{T}$ and the potential energy $\mathcal{U}$. The second type Lagrange equation is given by

$$\frac{d}{dt}\left(\frac{\partial \mathcal{L}}{\partial \dot{\boldsymbol{q}}}\right) - \frac{\partial \mathcal{L}}{\partial \boldsymbol{q}} = \boldsymbol{f}, \tag{2}$$

which describes the equation of motion of a multi-body system with the input forces $\boldsymbol{f}$. The kinetic energy consists of a rotatory and a translatory part, given by

$$\mathcal{T} = \frac{1}{2}\sum_{j=1}^{N} m_j ({}^0\dot{\boldsymbol{r}}_{j,C})^{T\,0}\dot{\boldsymbol{r}}_{j,C} + ({}^j\boldsymbol{\omega}_j)^{T\,j}\boldsymbol{J}_j{}^j\boldsymbol{\omega}_j \tag{3}$$

with the mass of the links m_j, the vector to the center of mass of each link, represented in the inertial frame ${}^0\boldsymbol{r}_{j,C}$, the angular rate ${}^j\boldsymbol{\omega}_j$ represented in the body fix frame and the inertia tensor ${}^j\boldsymbol{J}_j$ also represented in the body fix frame. The potential energy of the links is given by

$$\mathcal{U}_l = \sum_{j=1}^{N} m_j \boldsymbol{g}^T {}^0\boldsymbol{r}_{j,C} \tag{4}$$

with the gravity vector $\boldsymbol{g} = [0 \;\; 0 \;\; g]^T$. Another potential energy belongs to the elastic joints of the robot modeled as a spring damper system and given by

$$\mathcal{U}_f = \frac{1}{2}(\boldsymbol{q}_m - \boldsymbol{q}_a)^T \boldsymbol{K}(\boldsymbol{q}_m - \boldsymbol{q}_a) \tag{5}$$

with the diagonal stiffness matrix $\boldsymbol{K}$, the motor side positions $\boldsymbol{q}_m$ and the gearbox side positions $\boldsymbol{q}_a$. For the total potential energy it follows $\mathcal{U} = \mathcal{U}_l - \mathcal{U}_f$. The dissipative energy due to the damper is given by

$$F = \frac{1}{2}(\dot{\boldsymbol{q}}_m - \dot{\boldsymbol{q}}_a)^T \boldsymbol{D}(\dot{\boldsymbol{q}}_m - \dot{\boldsymbol{q}}_a) \tag{6}$$

with the diagonal damping matrix $\boldsymbol{D}$, the motor side velocities $\dot{\boldsymbol{q}}_m$ and the gearbox side velocities $\dot{\boldsymbol{q}}_a$.
The equations of motion are derived with the principle of d'Alembert and are given with

$$\frac{d}{dt}\left(\frac{\partial \mathcal{T}(\boldsymbol{q}, \dot{\boldsymbol{q}})}{\partial \dot{\boldsymbol{q}}}\right) - \frac{\partial \mathcal{T}(\boldsymbol{q}, \dot{\boldsymbol{q}})}{\partial \boldsymbol{q}} + \frac{\partial \mathcal{U}(\boldsymbol{q})}{\partial \boldsymbol{q}} + \frac{\partial F(\dot{\boldsymbol{q}})}{\partial \dot{\boldsymbol{q}}} = \boldsymbol{\tau}. \tag{7}$$

After calculation and sorting the equations of motion are given by

$$\boldsymbol{M}(\boldsymbol{q}_a)\ddot{\boldsymbol{q}}_a + \boldsymbol{c}(\boldsymbol{q}_a, \dot{\boldsymbol{q}}_a) + \boldsymbol{g}^*(\boldsymbol{q}_a) = \boldsymbol{K}(\boldsymbol{q}_m - \boldsymbol{q}_a) + \boldsymbol{D}(\dot{\boldsymbol{q}}_m - \dot{\boldsymbol{q}}_a), \tag{8}$$

$$\boldsymbol{J}_m\ddot{\boldsymbol{q}}_m + \boldsymbol{K}(\boldsymbol{q}_m - \boldsymbol{q}_a) + \boldsymbol{D}(\dot{\boldsymbol{q}}_m - \dot{\boldsymbol{q}}_a) = \boldsymbol{\tau} \tag{9}$$

with the mass matrix $\boldsymbol{M}$, the vector of Coriolis and centrifugal forces $\boldsymbol{c}$, the vector of gravity $\boldsymbol{g}^*$, the stiffness matrix $\boldsymbol{K}$, the damping matrix $\boldsymbol{D}$, and the diagonal matrix of the moments of inertia of the motors $\boldsymbol{J}_m$ and the command torques $\boldsymbol{\tau}$ to the motors.

2.1 Special case: Axis 1 system

For this special case all other joints are fixed and rigid. For the observer design the system is given in the state space representation in the states $\boldsymbol{x} = [q_a \;\; \dot{q}_a \;\; q_m^t \;\; \dot{q}_m^t]^T$

$$\dot{\boldsymbol{x}} = \begin{bmatrix} 0 & 1 & 0 & 0 \\ -\frac{k}{J_a} & -\frac{d}{J_a} & \frac{k}{J_a} & \frac{d}{J_a} \\ 0 & 0 & 0 & 1 \\ \frac{k}{J_m^t} & \frac{d}{J_m^t} & -\frac{k}{J_m^t} & -\frac{d}{J_m^t} \end{bmatrix} \boldsymbol{x} + \begin{bmatrix} 0 \\ 0 \\ 0 \\ \frac{1}{J_m^t} \end{bmatrix} \tau^t, \tag{10}$$

$$y = [0 \;\; 0 \;\; 1 \;\; 0]\,\boldsymbol{x} + 0d \tag{11}$$

with the damping coefficient d, the stiffnes coefficient c and with the motor sizes $J_m^t = u_0^2 J_m$, $q_m^t = \frac{q_m}{u_0}$, $\tau^t = \tau u_0$ which are transformed to the gearbox side with the gearbox ratio u_0.

2.2 Special case: Axis 2/3 system

The state space representation of the MIMO system is given by

$$\dot{\boldsymbol{x}} = \boldsymbol{A}(\boldsymbol{M})\boldsymbol{x} + \boldsymbol{B}\boldsymbol{\tau} + \tilde{\boldsymbol{C}}, \tag{12}$$

$$\boldsymbol{q}_m = \boldsymbol{C}\boldsymbol{x} \tag{13}$$

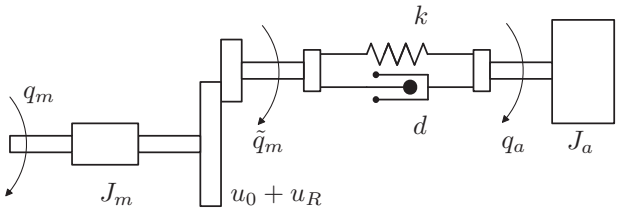

Fig. 2. Gearbox as a two mass spring damper system with nonideal ratio.

in the states $\boldsymbol{x} = \left[q_{a,2} \;\; \dot{q}_{a,2} \;\; q_{m,2}^t \;\; \dot{q}_{m,2}^t \;\; q_{a,3} \;\; \dot{q}_{a,3} \;\; q_{m,3}^t \;\; \dot{q}_{m,3}^t\right]^T$ and the parameter variant dynamic matrix

$$\boldsymbol{A} = \begin{bmatrix} 0 & 1 & 0 & 0 & 0 & 0 & 0 & 0 \\ \frac{-k_2}{m_{22}} & \frac{-d_2}{m_{22}} & \frac{k_2}{m_{22}} & \frac{d_2}{m_{22}} & \frac{-k_3}{m_{23}} & \frac{-d_3}{m_{23}} & \frac{k_3}{m_{23}} & \frac{d_3}{m_{23}} \\ 0 & 0 & 0 & 1 & 0 & 0 & 0 & 0 \\ \frac{k_2}{J_{m,2}^t} & \frac{d_2}{J_{m,2}^t} & \frac{-k_2}{J_{m,2}^t} & \frac{-d_2}{J_{m,2}^t} & 0 & 0 & 0 & 0 \\ 0 & 0 & 0 & 0 & 0 & 1 & 0 & 0 \\ \frac{-k_2}{m_{32}} & \frac{-d_2}{m_{32}} & \frac{k_2}{m_{32}} & \frac{d_2}{m_{32}} & \frac{-k_3}{m_{33}} & \frac{-d_3}{m_{33}} & \frac{k_3}{m_{33}} & \frac{d_3}{m_{33}} \\ 0 & 0 & 0 & 0 & 0 & 0 & 0 & 1 \\ 0 & 0 & 0 & 0 & \frac{k_3}{J_{m,3}^t} & \frac{d_3}{J_{m,3}^t} & \frac{-k_3}{J_{m,3}^t} & \frac{-d_3}{J_{m,3}^t} \end{bmatrix}, \tag{14}$$

with $m_{ij} = \frac{1}{\boldsymbol{M}^{-1}_{(i,j)}}$ and the input matrix

$$\boldsymbol{B} = \begin{bmatrix} 0 & 0 & 0 & \frac{1}{J_{m,2}^t} & 0 & 0 & 0 & 0 \\ 0 & 0 & 0 & 0 & 0 & 0 & 0 & \frac{1}{J_{m,3}^t} \end{bmatrix}^T, \tag{15}$$

the output matrix

$$\boldsymbol{C} = \begin{bmatrix} 0 & 0 & 1 & 0 & 0 & 0 & 0 & 0 \\ 0 & 0 & 0 & 0 & 0 & 0 & 1 & 0 \end{bmatrix}, \tag{16}$$

the feedthrough matrix

$$\boldsymbol{D} = \boldsymbol{0} \tag{17}$$

and the vector of the nonlinearities

$$\tilde{\boldsymbol{C}} = \begin{bmatrix} 0 \\ \boldsymbol{M}^{-1}_{(2,i)}\left(-\boldsymbol{c}(\boldsymbol{q}_a, \dot{\boldsymbol{q}}_a) - \boldsymbol{g}^*(\boldsymbol{q}_a)\right) \\ \boldsymbol{0} \\ 0 \\ \boldsymbol{M}^{-1}_{(3,i)}\left(-\boldsymbol{c}(\boldsymbol{q}_a, \dot{\boldsymbol{q}}_a) - \boldsymbol{g}^*(\boldsymbol{q}_a)\right) \\ \boldsymbol{0} \end{bmatrix}. \tag{18}$$

3. MODELING OF A GEARBOX WITH NON IDEAL RATIO

Many robots have a gearbox with a high ratio, due to the high rotating motors, which produce a low torque. Often harmonic drive or cycloid gearboxes are used. These gearbox types are complicated to model and can only be analyzed exactly with FEM programs. The resulting models are very big and so not useful for control design. So analogous models are derived which describe the system behavior in a sufficient way. For this reason the gearbox is modeled with a sinusoidal ratio, given by

$$\begin{aligned} u(q_m) &= u_0 + \sum_{j=1}^{N} m_N \cos\left(\frac{N}{u_0} q_m + \varphi_N\right) \\ &= u_0 + u_R \end{aligned} \tag{19}$$

with the basis ratio u_0, the frequency N the magnitude m_N and the phase φ_N. Due to energy consideratios the velocity is

$$\dot{q}_m = u(q_m)\dot{\tilde{q}}_m. \tag{20}$$

With integration of equation (20) it follows for the positions

$$q_m(q_m) = u_0\tilde{q}_m + \sum_{j=1}^{N} \frac{m_N}{N}\sin(\frac{N}{u_0}q_m + \varphi_N) + u_C. \tag{21}$$

3.1 The axis 1 model with a nonideal gearbox

The non ideal ratio is combined with the differential equation of the axis 1 system. The resulting nonlinear differential equation are given by

$$J_a\ddot{q}_a + k(q_a - \tilde{q}_m) + d(\dot{q}_a - \dot{\tilde{q}}_m) = 0, \tag{22}$$

$$J_m\ddot{q}_m u - k(q_a - \tilde{q}_m) - d(\dot{q}_a - \dot{\tilde{q}}_m) = \tau u, \tag{23}$$

which makes clear that the nonlinearity is acting on position, velocity and torque. Still this equation can be transformed into a nonlinear state space model in the states $\boldsymbol{x} = [q_a \;\; \dot{q}_a \;\; q_m \;\; \dot{q}_m]$ and given by

$$\dot{x}_1 = x_2, \tag{24}$$

$$\dot{x}_2 = -\frac{k}{J_a}x_1 - \frac{d}{J_a}x_2 + \frac{k}{J_a}\tilde{x}_3 + \frac{d}{J_a u}x_4, \tag{25}$$

$$\dot{x}_3 = x_4, \tag{26}$$

$$\dot{x}_4 = \frac{k}{J_m u}x_1 + \frac{d}{J_m u}x_2 - \frac{k}{J_m u}\tilde{x}_3 - \frac{d}{J_m u^2}x_4 + \frac{\tau}{J_m}, \tag{27}$$

with the auxiliary sizes

$$\tilde{x}_3 = \frac{1}{u_0}(x_3 - \frac{m_N}{N}\sin(Nx_3 + \varphi_N)), \tag{28}$$

$$u = u_0 + m_N\cos(Nx_3 + \varphi_N). \tag{29}$$

These state space model is later used for the observer design.

3.2 The axis 2/3 model with a nonideal gearbox

The MIMO model is derived with the help of equations (14) - (17). The result is given by

$$\dot{x}_1 = x_2, \tag{30}$$

$$\begin{aligned}\dot{x}_2 = &-\frac{k_2}{m_{22}}x_1 - \frac{d_2}{m_{22}}x_2 + \frac{k_2}{m_{22}}\tilde{x}_3 + \frac{1}{u_2}\frac{d_2}{m_{22}}x_4 \\ &- \frac{k_3}{m_{23}}x_5 - \frac{d_3}{m_{23}}x_6 + \frac{k_3}{m_{23}}\tilde{x}_7 + \frac{1}{u_3}\frac{d_3}{m_{23}}x_8 + \tilde{\boldsymbol{C}}_{(2)},\end{aligned} \tag{31}$$

$$\dot{x}_3 = x_4, \tag{32}$$

$$\dot{x}_4 = \frac{k_2}{J_{m,2}u_2}x_1 + \frac{d_2}{J_{m,2}u_2}x_2 - \frac{k_2}{J_{m,2}u_2}\tilde{x}_3 - \frac{d_2}{J_{m,2}u_2^2}x_4 + \frac{\tau_2}{J_{m,2}}, \tag{33}$$

$$\dot{x}_5 = x_6, \tag{34}$$

$$\begin{aligned}\dot{x}_6 = &-\frac{k_2}{m_{32}}x_1 - \frac{d_2}{m_{32}}x_2 + \frac{k_2}{m_{32}}\tilde{x}_3 + \frac{1}{u_2}\frac{d_2}{m_{32}}x_4 \\ &- \frac{k_3}{m_{33}}x_5 - \frac{d_3}{m_{33}}x_6 + \frac{k_3}{m_{33}}\tilde{x}_7 + \frac{1}{u_3}\frac{d_3}{m_{33}}x_8 + \tilde{\boldsymbol{C}}_{(6)},\end{aligned} \tag{35}$$

$$\dot{x}_7 = x_8, \tag{36}$$

$$\dot{x}_8 = \frac{k_3}{J_{m,3}u_3}x_5 + \frac{d_3}{J_{m,3}u_3}x_6 - \frac{k_3}{J_{m,3}u_2}\tilde{x}_7 - \frac{d_3}{J_{m,3}u_3^2}x_8 + \frac{\tau_3}{J_{m,3}}, \tag{37}$$

with the auxiliary sizes

$$\tilde{x}_3 = \frac{1}{u_0}(x_3 - \frac{m_N}{N}\sin(Nx_3 + \varphi_N)), \tag{38}$$

$$\tilde{x}_7 = \frac{1}{u_0}(x_7 - \frac{m_N}{N}\sin(Nx_7 + \varphi_N)), \tag{39}$$

$$u_2 = u_0 + m_N\cos(Nx_3 + \varphi_N), \tag{40}$$

$$u_3 = u_0 + m_N\cos(Nx_7 + \varphi_N). \tag{41}$$

4. STATE SPACE OBSERVER WITH AN INTERNAL MODEL

The task is to design an observer for a nonlinear coupled MIMO system. The work of Kurze [2008] showed that even for an observer, which does not have an internal model of the non ideal ratio, it is not possible to design a standard nonlinear observer. So we design an observer with linear tools and compensate for the nonlinearities.

For a linear SISO system a Luenberger observer can be used given by

$$\dot{\hat{\boldsymbol{x}}} = \boldsymbol{A}\hat{\boldsymbol{x}} + \boldsymbol{b}\tau^t + \boldsymbol{l}(q_m^t - \boldsymbol{c}^T\hat{\boldsymbol{x}}), \tag{42}$$

$$\hat{\boldsymbol{y}} = \hat{\boldsymbol{x}}. \tag{43}$$

If the observer has an internal model of the disturbance the extended observer equations are given by

$$\begin{bmatrix}\dot{\hat{\boldsymbol{x}}} \\ \dot{\hat{\boldsymbol{x}}}_s\end{bmatrix} = \begin{bmatrix}\boldsymbol{A} & \boldsymbol{E}\boldsymbol{C}_s \\ \boldsymbol{0} & \boldsymbol{A}_s\end{bmatrix}\begin{bmatrix}\boldsymbol{x} \\ \boldsymbol{x}_s\end{bmatrix} + \begin{bmatrix}\boldsymbol{b} \\ \boldsymbol{0}\end{bmatrix}\tau^t + \boldsymbol{l}(q_m^t - \boldsymbol{c}^T\hat{\boldsymbol{x}}), \tag{44}$$

$$\hat{\boldsymbol{y}} = \hat{\boldsymbol{x}}, \tag{45}$$

where $\boldsymbol{E}$ is a matrix, which results of the system equations. For a constant disturbance the internal model is given by

$$A_s = 0. \tag{46}$$

For a constant disturbance the internal model is given by $\ddot{x}_s + \omega_d^2 x_s = 0$ which is transformed into state space and given by

$$\dot{\boldsymbol{x}}_s = \begin{bmatrix}0 & \omega_d \\ -\omega_d & 0\end{bmatrix}\boldsymbol{x}_s, \tag{47}$$

$$y_s = [1 \;\; 0]\,\boldsymbol{x}_s, \tag{48}$$

with the frequency of the disturbance ω_d.

4.1 SISO observer for the nonlinear gearbox (axis 1)

Since the observer is linear and the system is nonlinear two assumptions are made.

Assumption 1. It is acceptable that the disturbance is a function of states and not a real external disturbance.

Assumption 2. The nonlinearity (disturbance) is acting only on the position level, thus the nonlinear ratio is fixed by $u = u_0$.

With the help of the equations (24) - (27) the observer, given by the equations (42) and (43), is implemented with

$$\boldsymbol{A} = \begin{bmatrix}0 & 1 & 0 & 0 & 0 & 0 & 0 \\ -\frac{k}{J_a} & -\frac{d}{J_a} & \frac{k}{J_a} & \frac{d}{J_a} & 0 & \frac{k}{J_a} & 0 \\ 0 & 0 & 0 & 1 & 0 & 0 & 0 \\ \frac{k}{J_m^t} & \frac{d}{J_m^t} & -\frac{k}{J_m^t} & -\frac{d}{J_m^t} & -\frac{1}{J_m^t} & -\frac{k}{J_m^t} & 0 \\ 0 & 0 & 0 & 0 & 0 & 0 & 0 \\ 0 & 0 & 0 & 0 & 0 & 0 & \omega_d \\ 0 & 0 & 0 & 0 & 0 & -\omega_d & 0\end{bmatrix}, \tag{49}$$

$$\boldsymbol{b} = \begin{bmatrix}0 & 0 & 0 & \frac{1}{J_m^t} & 0 & 0 & 0\end{bmatrix}^T, \tag{50}$$

$$\boldsymbol{c}^T = [0 \;\; 0 \;\; 1 \;\; 0 \;\; 0 \;\; 0]\,. \tag{51}$$

4.2 MIMO observer for the nonlinear gearbox (axis 2/3)

An analytic pole placement is not possible for the MIMO observer, because the equations can not be solved anymore. For this reason, we calculate the observer matrix $\boldsymbol{L}$

at some working points where the angles of axis 2 and axis 3 vary. During the experiment we interpolate between the different $\boldsymbol{L}$ matrices and schedule the dynamic matrix $\boldsymbol{A}$ with the mass matrix $\boldsymbol{M}$. For the MIMO case two more assumptions are made

Assumption 3. The nonlinearities $\tilde{\boldsymbol{C}}$ can be neglected or compensated.

Assumption 4. The different observer matrices are smooth enough.

With the help of equations (30) - (37) it follows for the observer

$$\dot{\hat{\boldsymbol{x}}} = \begin{bmatrix} \boldsymbol{A}_{2,2} & \boldsymbol{A}_{2,3} \\ \boldsymbol{A}_{3,2} & \boldsymbol{A}_{3,3} \end{bmatrix}, \boldsymbol{x} + \boldsymbol{B}\boldsymbol{\tau}^t + \boldsymbol{L}(\boldsymbol{q}_m^t - \boldsymbol{C}\hat{\boldsymbol{x}}) + \tilde{\boldsymbol{C}} \quad (52)$$

$$\hat{\boldsymbol{y}} = \hat{\boldsymbol{x}}, \quad (53)$$

with the parts of the dynamic matrix

$$\boldsymbol{A}_{2,2} = \begin{bmatrix} 0 & 1 & 0 & 0 & 0 & 0 & 0 \\ \frac{-k_2}{m_{22}} & \frac{-d_2}{m_{22}} & \frac{k_2}{m_{22}} & \frac{d_2}{m_{22}} & 0 & \frac{k_2}{m_{22}} & 0 \\ 0 & 0 & 0 & 1 & 0 & 0 & 0 \\ \frac{k_2}{J^t_{m,2}} & \frac{d_2}{J^t_{m,2}} & \frac{-k_2}{J^t_{m,2}} & \frac{-d_2}{J^t_{m,2}} & \frac{-1}{J^t_{m,2}} & \frac{-k_2}{J^t_{m,2}} & 0 \\ 0 & 0 & 0 & 0 & 0 & 0 & 0 \\ 0 & 0 & 0 & 0 & 0 & 0 & \omega_{d,2} \\ 0 & 0 & 0 & 0 & 0 & -\omega_{d,2} & 0 \end{bmatrix}, \quad (54)$$

$$\boldsymbol{A}_{2,3} = \begin{bmatrix} 0 & 0 & 0 & 0 & 0 & 0 & 0 \\ \frac{-k_3}{m_{23}} & \frac{-d_3}{m_{23}} & \frac{k_3}{m_{23}} & \frac{d_3}{m_{23}} & 0 & \frac{k_3}{m_{23}} & 0 \\ 0 & 0 & 0 & 0 & 0 & 0 & 0 \\ 0 & 0 & 0 & 0 & 0 & 0 & 0 \\ 0 & 0 & 0 & 0 & 0 & 0 & 0 \\ 0 & 0 & 0 & 0 & 0 & 0 & 0 \\ 0 & 0 & 0 & 0 & 0 & 0 & 0 \end{bmatrix}, \quad (55)$$

$$\boldsymbol{A}_{3,2} = \begin{bmatrix} 0 & 0 & 0 & 0 & 0 & 0 & 0 \\ \frac{-k_2}{m_{32}} & \frac{-d_2}{m_{32}} & \frac{k_2}{m_{32}} & \frac{d_2}{m_{32}} & 0 & \frac{k_2}{m_{32}} & 0 \\ 0 & 0 & 0 & 0 & 0 & 0 & 0 \\ 0 & 0 & 0 & 0 & 0 & 0 & 0 \\ 0 & 0 & 0 & 0 & 0 & 0 & 0 \\ 0 & 0 & 0 & 0 & 0 & 0 & 0 \\ 0 & 0 & 0 & 0 & 0 & 0 & 0 \end{bmatrix}, \quad (56)$$

$$\boldsymbol{A}_{3,3} = \begin{bmatrix} 0 & 1 & 0 & 0 & 0 & 0 & 0 \\ \frac{-k_3}{m_{33}} & \frac{-d_3}{m_{33}} & \frac{k_3}{m_{33}} & \frac{d_3}{m_{33}} & 0 & \frac{k_3}{m_{33}} & 0 \\ 0 & 0 & 0 & 1 & 0 & 0 & 0 \\ \frac{k_3}{J^t_{m,3}} & \frac{d_3}{J^t_{m,3}} & \frac{-k_3}{J^t_{m,3}} & \frac{-d_3}{J^t_{m,3}} & \frac{-1}{J^t_{m,3}} & \frac{-k_3}{J^t_{m,3}} & 0 \\ 0 & 0 & 0 & 0 & 0 & 0 & 0 \\ 0 & 0 & 0 & 0 & 0 & 0 & \omega_{d,3} \\ 0 & 0 & 0 & 0 & 0 & -\omega_{d,3} & 0 \end{bmatrix}, \quad (57)$$

the input matrix

$$\boldsymbol{B} = \begin{bmatrix} 0 & 0 & 0 & \frac{1}{J^t_{m,2}} & 0 & 0 & 0 & 0 & 0 & 0 & 0 & 0 & 0 \\ 0 & 0 & 0 & 0 & 0 & 0 & 0 & 0 & 0 & \frac{1}{J^t_{m,3}} & 0 & 0 & 0 \end{bmatrix}^T \quad (58)$$

and the output matrix

$$\boldsymbol{C} = \begin{bmatrix} 0 & 0 & 1 & 0 & 0 & 0 & 0 & 0 & 0 & 0 & 0 & 0 & 0 \\ 0 & 0 & 0 & 0 & 0 & 0 & 0 & 0 & 0 & 1 & 0 & 0 & 0 \end{bmatrix}. \quad (59)$$

The Design with the LQR criteria is used to calculate the observer matrix $\boldsymbol{L}$, where the goal is to minimize the quality criterion

$$J = \frac{1}{2}\int_0^\infty (\boldsymbol{e}^T\boldsymbol{Q}\boldsymbol{e} + \boldsymbol{u}^T\boldsymbol{S}\boldsymbol{u})dt. \quad (60)$$

A solution of this equation is given by

$$\boldsymbol{u} = -\boldsymbol{L}\boldsymbol{e} = -\boldsymbol{S}^{-1}\boldsymbol{C}\boldsymbol{P}\boldsymbol{e}, \quad (61)$$

with the matrix $\boldsymbol{P}$ as a solution of the Riccati equation

$$\boldsymbol{A}\boldsymbol{P} + \boldsymbol{P}\boldsymbol{A}^T - \boldsymbol{P}\boldsymbol{C}^T\boldsymbol{S}^{-1}\boldsymbol{C}\boldsymbol{P} + \boldsymbol{Q} = \boldsymbol{0}. \quad (62)$$

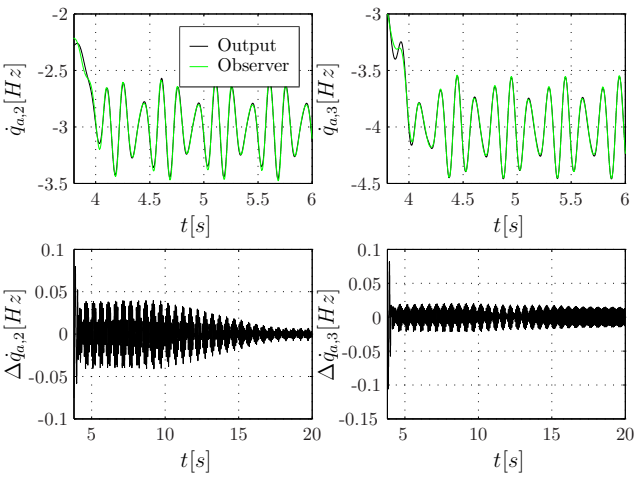

Fig. 3. Simulation results, where the system has a nonlinear ratio (only) on position level and the observer compensates for the nonlinearities $\tilde{\boldsymbol{C}}$.

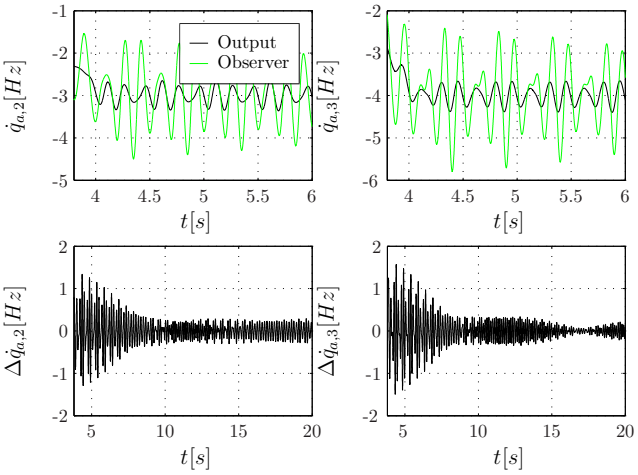

Fig. 4. Simulation results, where the the observer must handle the complete nonlinear system.

Simulation results of the MIMO observer are shown in the figures 3-4, where the system always gets more complicated. In figure 3 the observer shows a good convergence although the system has some nonlinearities. In figure 4 the observer does not convert in a sufficient way, due to the nonlinearities.

5. REJECTION OF THE GEARBOX RIPPLES

We present an observer based method and a method based on the measurement of gearbox side information.

5.1 Observer based algorithm for the SISO case (axis 1)

The observer based method is shown in figure 5, where the complete control system is visible.

For the derivation of the adaptive control law we interpret the nonlinearities (ripples) as external disturbances d_i acting on several levels i. At the output these disturbances are visible through the unknown transfer function $G_{x,i}$. Without an adaptive signal v and the disturbances d_i it

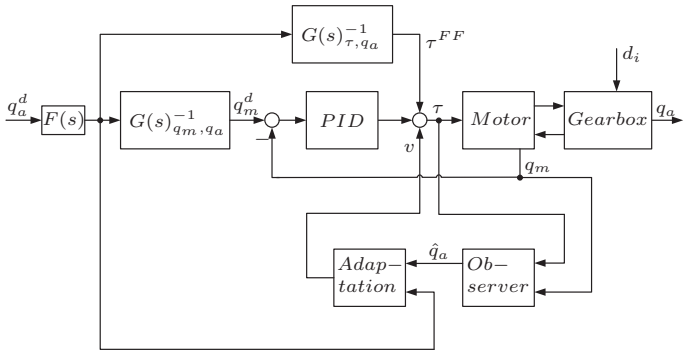

Fig. 5. Block diagram of the complete control system.

follows for the non measurable output $q_a = q_a^d$, if an ideal feedforward controller is used, which implements the inverse of the plant aside from the ripples. If the disturbance and the adaptive signal is added it follows

$$q_a = q_a^d + G_d v + \sum G_{x,i} d_i(q_a), \tag{63}$$

with the disturbance transfer function $G_d = \frac{q_a}{v}$. The transfer functions $G_{x,i}$ do not have any influence on the adaptation law. But it is important that the disturbances d_i have the same frequency. Since q_a is not measurable the observer state $\hat{q}_a$ is used in the adaptive algorithm.
Here the system has to be made fictive free from the reference trajectory which is obtained by

$$e = q_a - q_a^d. \tag{64}$$

For the adaptation error it holds

$$e(t) = \sum G_{x,i} d_i(q_a) + G_d[\boldsymbol{w}^T \boldsymbol{\theta}(t)], \tag{65}$$

which is minimized with a gradient steepest descend algorithm, given by

$$\boldsymbol{\theta}(t+1) = \boldsymbol{\theta}(t) - 2\mu G_d[\boldsymbol{w}^T e(t)] \tag{66}$$

with $\boldsymbol{w}^T = \begin{bmatrix} \cos(N\hat{q}_a) \\ \sin(N\hat{q}_a) \end{bmatrix}^T$ and the adaptive gain μ, which describes how fast the algorithm converts. The cancellation part is given by

$$v = \boldsymbol{w}^T \boldsymbol{\theta}(t). \tag{67}$$

Experimental results are shown in figure 6, where the magnitude of the ripple, see $\dot{q}_a$, is not constant. So the adaptive gain μ is chosen high enough to track these variations.
The comparison between the compensated and the uncompensated signal $\Delta\dot{q}_a = \dot{q}_a^d - \dot{q}_a$ shows the improvement of the algorithm. At the beginning of the movement both signals $\Delta\dot{q}_a$ are very similar, after 5s the adaptive algorithm converts and the gearbox ripples are rejected. A better impression of the improvement is shown in the frequency domain FFT spectra of the gearbox side velocity error $|\Delta\dot{q}_a|$. This spectra shows that the oscillation with $N = 2$ is rejected by a factor of 4, which was the goal of the algorithm.
This algorithm only works because the observer estimates the gearbox side states well enough, which shows the comparison between the observed gearbox side velocity $\frac{d}{dt}\hat{q}_a$ and the measured gearbox side velocity $\dot{q}_a$, which is not used in this algorithm.
The adaptive states $\boldsymbol{\theta}$ show a non constant behavior, because they have to track the variations in magnitude and phase.

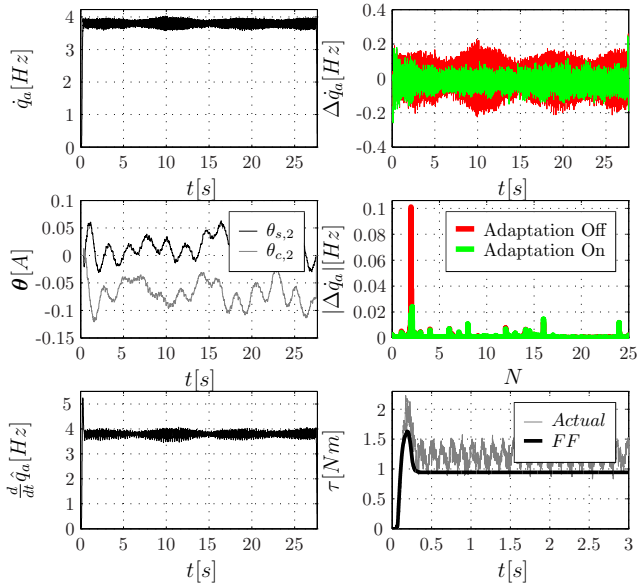

Fig. 6. Experimental results for gearbox ripple rejection with an observer based approach. The adaptive gain is $\mu = 1$ and the eigenvalues of the observer are $\boldsymbol{\lambda} = -60[\frac{rad}{s}]$.

5.2 Rate sensor based algorithm for the SISO case

The derivation of the adaptive control law is similar to the previous algorithm, beside for the error signal the measured gearbox side rate is used.
Without an adaptive signal v and the disturbances d_i it follows for the measurable output $\dot{q}_a = \dot{q}_a^d$, if an ideal feedforward controller is used, which implements the inverse of the plant aside from the ripples. If the disturbance and the adaptive signal is added it follows

$$\dot{q}_a = \dot{q}_a^d + G_d v + \sum G_{x,i} d_i(q_a). \tag{68}$$

For the adaptive algorithm the system has to be made fictive free from the reference trajectory which is obtained by

$$e = \dot{q}_a - \dot{q}_a^d. \tag{69}$$

For the adaptation error it holds

$$e(t) = \sum G_{x,i} d_i(q_a) + G_d[\boldsymbol{w}^T \boldsymbol{\theta}(t)], \tag{70}$$

which is minimized with a gradient steepest descend algorithm, given by

$$\boldsymbol{\theta}(t+1) = \boldsymbol{\theta}(t) - 2\mu G_d[\boldsymbol{w}^T e(t)] \tag{71}$$

with $\boldsymbol{w}^T = \begin{bmatrix} \cos(Nq_m) \\ \sin(Nq_m) \end{bmatrix}^T$ and the cancellation part is given in equation (67).

Experimental results are shown in figure 7, where the performance of the algorithm is very similar to the results shown in figure 6.

5.3 Rate sensor based MIMO algorithm (axis 2/3)

The derivation of the adaptive algorithm is similar to Wu and Bodson [2004], so here only the basis equations are given. For the output of the plant with an ideal feedforward controller it holds

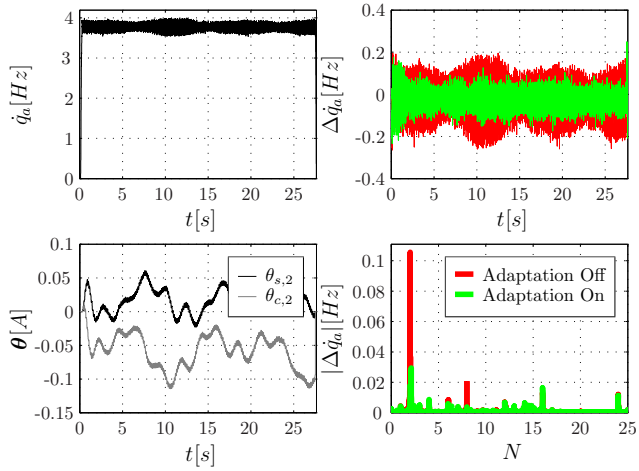

Fig. 7. Experimental results for gearbox ripple rejection with an rate sensor based approach for axis 1. The adaptive gain is $\mu = 1$.

$$\begin{bmatrix} \dot{q}_{a,2} \\ \dot{q}_{a,3} \end{bmatrix} = \begin{bmatrix} \dot{q}^d_{a,2} \\ \dot{q}^d_{a,3} \end{bmatrix} + \boldsymbol{G}_d \begin{bmatrix} v_2 \\ v_3 \end{bmatrix} + \sum \boldsymbol{G}_{x,i} \begin{bmatrix} d_{i,2} \\ d_{i,3} \end{bmatrix} \tag{72}$$

with $\boldsymbol{G}_d = \frac{\dot{\boldsymbol{q}}_a}{\boldsymbol{v}}$. The error of the adaptation is given by

$$\boldsymbol{e} = \dot{\boldsymbol{q}}_a - \dot{\boldsymbol{q}}^d_a \tag{73}$$

$$= \boldsymbol{G}_d \begin{bmatrix} \boldsymbol{\theta}_2(t)\boldsymbol{w}_2 \\ \boldsymbol{\theta}_3(t)\boldsymbol{w}_3 \end{bmatrix} + \sum \boldsymbol{G}_{x,i} \begin{bmatrix} d_{i,2} \\ d_{i,3} \end{bmatrix} \tag{74}$$

with $\boldsymbol{w}_i^T = \begin{bmatrix} \cos(Nq_{m,i}) \\ \sin(Nq_{m,i}) \end{bmatrix}^T$, which is minimized with a gradient steepest descend algorithm, given with sorted states

$$\begin{bmatrix} \boldsymbol{\theta}_c \\ \boldsymbol{\theta}_s \end{bmatrix} = -\mu \hat{\boldsymbol{G}}^{-1}(\omega_d, \boldsymbol{M}) \begin{bmatrix} \boldsymbol{e}(t)cos(Nq_m) \\ \boldsymbol{e}(t)sin(Nq_m) \end{bmatrix}, \tag{75}$$

with the scheduled inverse system matrix of the closed loop disturbance transfer function

$$\hat{\boldsymbol{G}}^{-1}(\omega_d, \boldsymbol{M}) = \begin{bmatrix} \Re\{\hat{\boldsymbol{G}}_d(j\omega_d)\} & \Im\{\hat{\boldsymbol{G}}_d(j\omega_d)\} \\ -\Im\{\hat{\boldsymbol{G}}_d(j\omega_d)\} & \Re\{\hat{\boldsymbol{G}}_d(j\omega_d)\} \end{bmatrix}. \tag{76}$$

Finally the adaptive feedforward cancellation is given by

$$\boldsymbol{v}_i = \boldsymbol{\theta}_i \boldsymbol{w}_i. \tag{77}$$

Experimental results are shown in figure 8. The best impression of the improvement is shown in the frequency domain FFT spectra of the gearbox side velocities $\dot{q}_{a_2}$ and $\dot{q}_{a_3}$. This spectra shows that the oscillation with $N = 2$ is rejected by a factor of 3, where all the other peaks or not influenced by the algorithm. The adaptive states are not constant because of many facts, like non constant magnitude or non constant moment of inertia.

6. CONCLUSION

We presented algorithms for gearbox ripple rejection on robots. The axis 1 problem can be solved with an observer, which is designed with linear tools, although the plant is nonlinear. This algorithm has the same performance as a rate sensor based algorithm, which needs an additional sensor, which is not volitional.
We also tried to design a MIMO observer for the gearbox ripple problem. This linear observer can handle some nonlinearities, but with the full nonlinear system the

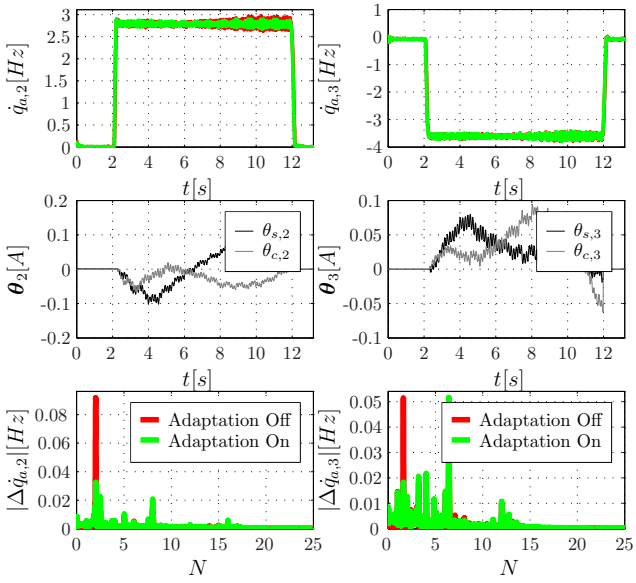

Fig. 8. Experimental results for gearbox ripple rejection with an rate sensor based approach for axis 2/3. The adaptive gain is $\mu = 1$.

magnitude of ripples are estimated to high. For this reason we implemented a rate sensor based algorithm, which rejects the ripple in a sufficient way.
For future work, we will work on the observer problem for the nonlinear MIMO case. One solution is to use nonlinear control theory or give the linear observer a more precise model of the disturbance.

REFERENCES

M. Bodson and S. C. Douglas. Adaptive algorithms for the rejection of sinusoidal disturbances with unknown frequency. *Automatica*, 33:2213–2221, 1997.

C. Bohn, H-J. Karkosch, and F. Svaricek. State observers for periodic signals: A case study in active vibration control. *Automatisierungstechnik*, 53, 2005.

C. C. de Wit, B. Siciliano, and G. Bastin. *Theory of Robot Control*. Springer Verlag, 1996.

X. Guo and M. Bodson. Equivalence between adaptive feedforward cancellation and disturbance rejection using the internal model principle. *Adaptive Control and Signal Processing*, 24:211–218, 2010.

M. Kurze. *Modellbasierte Regelung von Robotern mit elastischen Gelenken ohne abtriebsseitige Sensorik*. PhD thesis, TU Muenchen, 2008.

S. Maier and M. Bodson. Periodic disturbance rejection on a laser beam stabilizing system with adaptive controllers. In *Proc. International Conference on Noise and Vibration Control (ISMA)*, 2008.

F. Pfeiffer. *Einfuehrung in die Dynamik*. Teubner Studienbuecher, 1989.

M. W. Spong and M. Vidyasagar. *ROBOT DYNAMICS AND CONTROL*. John Wiley & Sons, 1989.

Sumitomo. Cyclo drive europe. *Serie Fine Cyclo*, 1996.

Teijin-Seiki. Catalogue rv-e series. 2010.

B. Wu and M. Bodson. Multi-channel active noise control for periodic sources-indirect approach. *Automatica*, 40: 203–212, 2004.